

Department of Physics, Chemistry and Biology

Master's Thesis

Search for Dark Matter in the Upgraded High Luminosity LHC at CERN

Impact of ATLAS phase II performance on a mono-jet analysis

Sven-Patrik Hallsjö

Thesis work performed at Stockholm University

Linköping, June 4, 2014

LITH-IFM-A-EX--14/2863--SE



**Linköpings universitet
TEKNISKA HÖGSKOLAN**

Department of Physics, Chemistry and Biology
Linköping University
SE-581 83 Linköping, Sweden

Department of Physics, Chemistry and Biology

Search for Dark Matter in the Upgraded High Luminosity LHC at CERN

Impact of ATLAS phase II performance on a mono-jet analysis

Sven-Patrik Hallsjö

Thesis work performed at Stockholm University

Linköping, June 4, 2014

Supervisor: **Docent Christophe Clément**
 FYSIKUM Stockholm University
Professor Magnus Johansson
 IFM, Linköping University

Examiner: **Professor Magnus Johansson**
 IFM, Linköping University



Avdelning, Institution
Division, Department

Theoretical physics group
Department of Physics, Chemistry and Biology
SE-581 83 Linköping

Datum
Date

2014-06-04

Språk
Language

Svenska/Swedish
 Engelska/English

Rapporttyp
Report category

Licentiatavhandling
 Examensarbete
 C-uppsats
 D-uppsats
 Övrig rapport

ISBN
—

ISRN
LITH-IFM-A-EX--14/2863--SE

Serietitel och serienummer
Title of series, numbering

ISSN
—

URL för elektronisk version

<http://urn.kb.se/resolve?urn=urn:nbn:se:liu:diva-XXXXXX>

Titel Sökandet efter mörk materia i den uppgraderade hög luminositets LHC i CERN
Title Search for Dark Matter in the Upgraded High Luminosity LHC at CERN

Undertitel Påverkan av ATLAS fas II prestanda på en mono-jet analys
Subtitle Impact of ATLAS phase II performance on a mono-jet analysis

Författare Sven-Patrik Hallsjö
Author

Sammanfattning
Abstract

Something as an introduction:

The LHC at CERN is undergoing an upgrade to increase the center of mass energy for the colliding particles which means that new physical processes will be explored. One drawback of this is that it will be harder to isolate unique particle collisions since more and more collisions will occur simultaneously, so called pile-up.

One hope for the upgrade is that WIMP models of dark matter will be detected.

This thesis covers looking at effective operators which try to explain dark matter without adding new theories to the standard model or QFT.

Some results and a slight conclusion.

Nyckelord

Keywords ATLAS, Beyond standard model physics, CERN, Dark matter, Elementary particle physics, High energy physics, something, this is in mythesis.sty

Abstract

Something as an introduction:

The LHC at CERN is undergoing an upgrade to increase the center of mass energy for the colliding particles which means that new physical processes will be explored. One drawback of this is that it will be harder to isolate unique particle collisions since more and more collisions will occur simultaneously, so called pile-up.

One hope for the upgrade is that WIMP models of dark matter will be detected.

This thesis covers looking at effective operators which try to explain dark matter without adding new theories to the standard model or QFT.

Some results and a slight conclusion.

Acknowledgments

I wish to dedicate this thesis to my mathematics teacher Ulf Rydmark without whom I would not have studied physics.

A big thank you to my family, fiancée and friends who have supported me throughout my education. A warm thank you to my friend Joakim Skoog who altered some of the images for me.

I want to thank my supervisor Christophe Clément and all those who helped me at Stockholm University.

I also want to thank my examiner Magnus Johansson, who always took time to answer any question from and support his students.

A special thank you to Professor Irina Yakimenko without whom my master years would have been duller and probably impossible.

Finally I want to thank someone someone for proofreading my

*Linköping, June 2014
Sven-Patrik Hallsjö*

Contents

Notation	ix
1 Introduction	1
1.1 Research goals	2
1.2 Theoretical Background	3
1.2.1 Quantum mechanics and quantum field theory	3
1.2.2 Nuclear, particle and subatomic particle physics	4
1.2.3 The standard model of particle physics	4
1.2.4 Dark matter	5
1.2.5 Effective field theory	6
1.2.6 Search for WIMPS	8
1.3 Experimental overview	10
1.3.1 LHC	10
1.3.2 ATLAS	11
1.3.3 Coordinate system	12
1.3.4 Reconstructing data	12
1.3.5 Pile-up	13
1.3.6 Mono-jet analysis	13
1.3.7 Phase II high luminosity upgrade	14
1.3.8 Monte Carlo simulation	15
2 Validation of smearing functions	17
2.1 Smearing functions	18
2.2 Validation	19
2.3 Results	20
2.3.1 Electron and photon	21
2.3.2 Muon	22
2.3.3 Tau	22
2.3.4 Jets	23
2.3.5 Missing Transversal Energy	24
2.4 Expected results	25
2.5 Discussion	27
2.5.1 Smearing independent on pile-up	27

2.5.2 Comparison to expected results	27
2.6 Conclusion	28
3 Evaluating dark matter signals	29
3.1 Signal to background ratio	29
3.1.1 Selection criteria	30
3.1.2 Verifying background data	30
3.1.3 Figures of merit	31
3.1.4 D5 operators	32
3.1.5 Light vector mediator models	32
3.1.6 Susy models?	32
3.2 Other selection criteria and observables	32
3.3 Mitigating the effect of the high luminosity	32
3.4 Results	33
3.4.1 Limit on M^*	33
3.4.2 Effect of pile-up on M^*	33
3.4.3 Previous results	34
3.4.4 Limit on mediator mass	34
3.4.5 Effect of pile-up on mediator mass	34
3.5 Discussion	34
3.6 Conclusion	34
4 Results and Conclusions	35
4.1 Validation of smearing functions	35
4.2 Signal to background ratio	35
4.2.1 Limit on M^*	35
4.2.2 Limit on mediator mass	35
4.3 Other selection criteria and observables	35
4.3.1 Limit on M^*	35
4.3.2 Limit on mediator mass	35
4.4 Mitigating the effect of the high luminosity	35
4.5 Recommendations to mitigate the effect of the high luminosity . .	35
4.6 Suggestions for future research	36
A Datasets	39
A.1 Background processes	39
A.1.1 Validation	39
A.1.2 Background to signals	39
A.2 D5 signal processes	40
A.3 Light vector mediator processes	40
Bibliography	45

Notation

NOTATIONS

Notation	Explanation
barn(b)	1 barn(b)= 10^{-24} cm ²
\oplus	$a \oplus b = \sqrt{a^2 + b^2}$, $a \oplus b \oplus c = \sqrt{a^2 + b^2 + c^2}$

ABBREVIATIONS

Abbreviation	Expansion
ATLAS	A large Toroidal LHC ApparatuS
CERN	Organisation européenne pour la recherche nucléaire ¹
CMS	Compact Muon Solenoid
LHC	Large Hadron Collider
RMS	Root Mean Square
SM	the Standard Model of particle physics
WIMP	Weakly Interacting Massive Particle
WIMPS	Weakly Interacting Massive ParticleS
QED	Quantum ElectroDynamics
QFT	Quantum Field Theory
QM	Quantum Mechanics

¹Originally, Conseil Européen pour la Recherche Nucléaire

1

Introduction

Discrepancies in measurements of the rotations of galaxies indicate the presence of a large amount of matter which interacts through gravity, though not electromagnetically making it invisible to our telescopes. This matter is commonly referred to as dark matter. Since no known or hypothesised particle in the standard model of particle physics can be used as a candidate for dark matter, this hints at the presence of new physics.

At the Organisation Européene pour la Recherche Nucléaire (CERN) focus now lies to discover any evidence of so called weakly interacting massive particles (WIMPS) which may be a candidate for dark matter. It is usually impossible to detect any interaction of dark matter candidates on the subatomic scale, however through looking at proposed interactions, searching for assumed decay channels and by investigating what is invisible to the detectors by using momentum conservation it is hoped that signs will be found. Though to date, none have been found.

Both experiments and current theories now show that higher energies are required at the LHC to be able to see any signs. This is why the LHC and all detectors are undergoing a vast upgrade program [1]. In this thesis focus will be on the last part of the upgrade due for completion in 2023, known as the high luminosity-LHC phase II upgrade; and also on the ATLAS detector. The method used in this thesis focuses on looking at data which emulate conditions at the upgraded LHC.

1.1 Research goals

This research took place at Stockholm University from January 7th until **when?** During the research period the following tasks were set up and performed/answered:

- Implement a C++ programme that loops over the collisions inside the signal and background datasets.
- For each collision retrieve the relevant observables (variables used to extract the signal over the background) and apply "smearing functions" to emulate the effect of the high luminosity on the observables.
- For both signal and background datasets, compare observables before and after smearing. What observables are the least/most affected?
- Implement selection criteria that selects the signal collisions efficiently while reduces significantly the background. In a first step the selection criteria should be taken from existing studies.
- Selection criteria can be evaluated and compared with each other using a figure of merit P , that measures the sensitivity of the experiment to the dark matter signal. Calculate P for the given selection criteria before and after smearing.
- What is the effect of the high luminosity (smearing) on the value of P ?
- Investigate other selection criteria and observables, to mitigate the effect of high luminosity. Use P to rank different criteria after smearing.
- Conclude on the effect of the high luminosity on the sensitivity for dark matter and possible ways to mitigate its effects using alternative observables and selection criteria.

1.2 Theoretical Background

1.2.1 Quantum mechanics and quantum field theory

In the beginning of the 20th century, some physical phenomena could not be explained by classical physics, for example the ultra-violet disaster of any classical model of black-body radiation, and the photoelectric effect [2]. It was these phenomena that led to the formulation of quantum mechanics (QM), where energy transfer is quantized and particles can act as both waves and particles at the same time [3].

Combining QM with classical electromagnetism proved harder than expected, colliding a photon(em-field) and an electron (particle/wave) is quite tricky. This can be seen when trying to calculate the scattering between them both in a QM schema. One idea that came from this was to explain them both in the same framework, field theory. Also, trying to incorporate special relativity into QM suggested a field description where space-time is described using the metric formalism from differential geometry. The culmination of both of these problems is the first part of a Quantum field theory (QFT), Quantum electrodynamics (QED) which with incredible precision explains electromagnetic phenomena including effects from special relativity[4]. It is in this merging that antimatter was theorised, since it is a requirement for the theory to hold. After the discovery of antimatter, the theory was set in stone. Since this the theory has been altered somewhat to explain more and more experimental data. This is discussed more in subsection 1.2.2 and subsection 1.2.3.

To be able to calculate properties in QFT one uses the Lagrangian formalism [5], which gives a governing equation for the different physical processes. In general the Lagrangian used for the Standard model is quite complicated, one can thus focus on one of the different terms corresponding to a specific interaction. This can be done to calculate the so called cross-section for a process, which is related to the probability that that process will occur. A step to simplify the calculations is to use the so called Feynman diagrams, an example of which is given in figure 1.1.

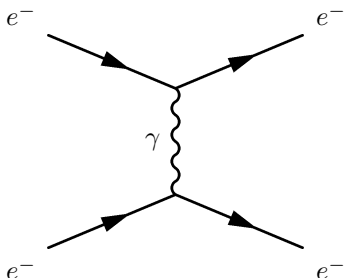


Figure 1.1: An example of a Feynman diagram explaining an electron-electron scattering using QED.

Through the figure, which comes with certain rules, and knowing what the major process (in this case QED) one can calculate the cross-section [4]. It is this that is needed to predict what one will be able to detect new particles.

1.2.2 Nuclear, particle and subatomic particle physics

Many could argue that these branches of physics started after Ernest Rutherford famous gold foil experiment [6], where he discovered that matter is composed of matter with a nucleus, a lot of empty space and electrons.

It was this that sparked the curiosity to see what the nucleus is made of and what forces govern the insides of atoms. After this, and the combination of the theoretical description given by QM, a lot more has been discovered and still more has been predicted. The newest of these is of course the Higgs particle, which was predicted through QFT and then discovered by the ATLAS and the CMS experiments at CERN [7].

The discovered particles are often divided into different groups depending on the fundamental particles that build them up. For instance, particles build up of three quarks are known as hadrons. Particles with an integer spin are known as bosons whereas half-integer particles are known as fermions.

1.2.3 The standard model of particle physics

The standard model of particle physics, referred to simply as the standard model (SM), is the particle zoo which tries to categorize all the particles and that have been discovered experimentally. QFT explains the interactions between these particles and it has also predicted several particles by including symmetries [6]. Regarding SM, Gauge bosons are the force carriers for the different forces, quarks are the and leptons are the fundamental blocks that we know of so far. The difference between the later two is if they interact via the strong force or not.

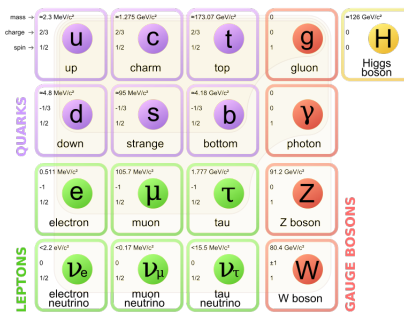


Figure 1.2: The standard model of particle physics where the three first columns represent the so called generations, starting with the first. [8].

SM is today the pinnacle of particle physics and can be used to explain almost everything that occurs around us. There are however some problems [9]:

- No QFT for general relativity! There is no link between gravity and the SM.
- Asymmetry between matter and antimatter can not be fully explained.
- No dark matter candidate!
- No explanation that can contain dark matter.

In this thesis focus lies with dark matter, some more introduction to possible dark matter and different candidates in extensions to SM are explained in subsection 1.2.4.

1.2.4 Dark matter

Dark matter is among other things, the name given to the solution to the discrepancies of galactic rotations.

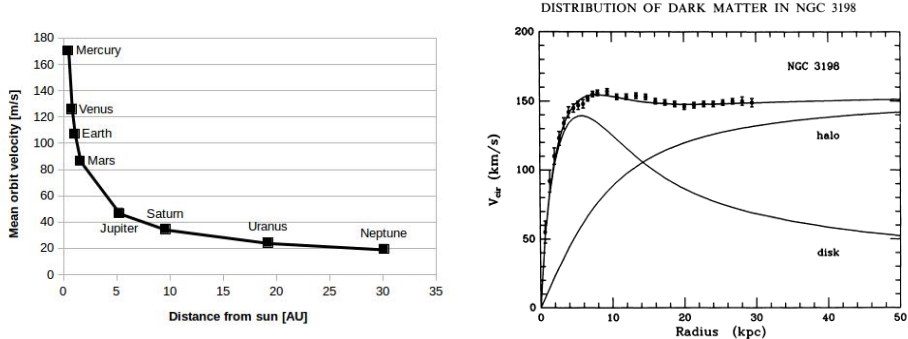
To explain this, focus on matter in a galaxy which are rotating around the center of the galaxy. Through Newtons law of gravity and the centrifugal force one can calculate the rotation speed dependent on the distance to the center of the galaxy. Since one of these forces is attractive and the other repulsive, if the matter is in a stable orbit around the galactic center (which they are) they must be equal and give us an expression for the speed depending on the distance. Newtons law can be written as the following:

$$F_{Gravitational} = G \frac{Mm}{r^2} = G_M \frac{m}{r^2} \quad F_{Centrifugal} = m \frac{V^2}{r} \quad (1.1)$$

where G is the gravitational constant, M the mass of the centre object, m the mass of the matter, r the distance between the two and V is the rotation speed. It has been simplified using G_M since all matter orbits the same galactic center. Setting the equations in (1.1) results in:

$$G_M \frac{m}{r^2} = m \frac{V^2}{r} \Leftrightarrow V^2 = \frac{G_M}{r} \Rightarrow V = \sqrt{\frac{G_M}{r}} \propto \frac{1}{\sqrt{r}} \quad (1.2)$$

where the speed is assumed to be positive and \propto means proportional. Through these simple calculations it shown that the rotation speed should decrease with increased distance. The same reasoning can be applied to our solar system where this is the case figure 1.3a. The relation in these units is $V = \frac{107}{\sqrt{r}}$ where 107 can be used in (1.2) to calculate the mass of the sun. However when looking at galaxies, even when taking into account that one has to see the galaxies as a mass distribution and that the above is only true when outside of the inner mass half, this is not the case! In figure 1.3b experimental data can be seen from the galaxy NGC3198 with a fitted curve which does not decrease with the distance but is instead constant. This is the discrepancy which is solved by postulating the existence of dark matter. After this the big question arises, what could this dark matter consist of? What is known so far lies in the name. It is called dark since no electromagnetic interaction and matter since gravitational interaction. This means that it can not be made up of any baryonic matter or anything in the Standard Model apart from neutrinos. The main interest of this thesis and also the main contributor to the rotational discrepancies is known as cold dark matter. This is due to the matter having a low speed, thus low kinetic energy, and have a high particle mass (In the GeV scale) [9, 12, 13]. This means however that neutrinos can not be a candidate, thus dark matter can not be made out of any standard model particles. There are several ideas to detected dark matter, [9]



(a) *Rotation speed of planets in our solar system. Since the distance is quite small on an astronomical scale, there is no sign of dark matter. Based on data from [10].*

(b) *Rotation speed of matter in NGC3198 with a curve fitting and three different models, if only a dark model halo existed, if there was no dark matter and the correct, if both exist [11].*

Figure 1.3: Different rotation curves, both for planets in our solar system and matter in the NGC3198 galaxy.

- Ordinary matter interacting with ordinary matter can produce dark matter, known as production. Which is the processes that occurs at particle accelerators.
- Dark matter interacting with ordinary matter can produce dark matter, known as direct detection.
- Dark matter interacting with dark matter can produce ordinary matter, known as indirect detection.

In this thesis the focus lies with production. There are several theories how to detect dark matter in proton-proton collisions such that occur at the LHC at CERN this is covered more in subsection 1.2.6.

1.2.5 Effective field theory

In quantum field theory the objective is usually to find the part of the Lagrangian which explains a type of interaction, known as the operator of the interaction and also to find the probability amplitude (cross-section) for a certain interaction. For complicated processes it is easier to employ certain conditions so that the small scale phenomena are simplified and the whole picture understood. This is known as using an effective field theory and the idea can be seen in figure 1.4. The operator can be found through assuming the possible interactions and using the effective field theory [4]. The cross-sections can be found through the Feynman diagrams as described in subsection 1.2.1.

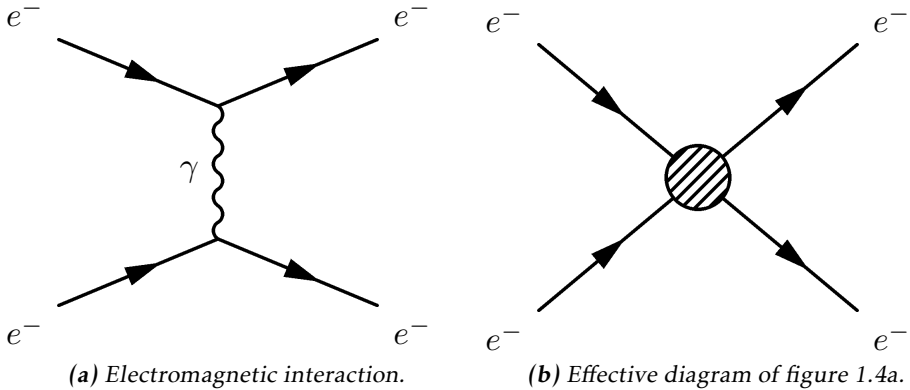


Figure 1.4: Feynman diagram of an electron-electron scattering, both as an ordinary diagram and as its effective theory version, where the details are hidden in the blob.

In this thesis the same effective field theory as in Refs. [12, 14] will be considered. The WIMP (usually denoted χ) is assumed to be the only particle in addition to the standard model fields. χ will be assumed odd under some Z_2 symmetry. This means that an even number of χ must be in every coupling. It is assumed that the whatever mediator exists is heavier than the WIMPS, meaning that their interactions are in higher order terms of the effective field theory and thus not included in the operators. For simplicity, the WIMPS are assumed to be SM singlets, thus invariant under SM gauge transformations, and the coupling to the Higgs boson is neglected.

The focus for the operators will be quark bilinear operators on the form $\bar{q}\Gamma q$ where Γ is a 4×4 matrix of the complete set,

$$\Gamma = \{1, \gamma^5, \gamma^\mu, \gamma^\mu \gamma^5, \sigma^{\mu\nu}\} \quad (1.3)$$

This will dictate how the operators are written, more of why this is done can be found in [4, 12, 14].

This, together with the coupling with the strong force defines an effective field theory of the interaction of singlet WIMPS with hadronic matter. It is a non-renormalizable field theory which will break down when the mediator mass is close to the mass of the WIMP. The condition for this is derived in [14] and gives:

$$M > 2m_\chi \quad (1.4)$$

where m_χ is the mass of the WIMP and M is the mass of the mediator. There is also the requirement that:

$$M \lesssim 4\pi M_* \quad (1.5)$$

where M_* is the energy scale where the effective theory is no longer a good ap-

proximation.

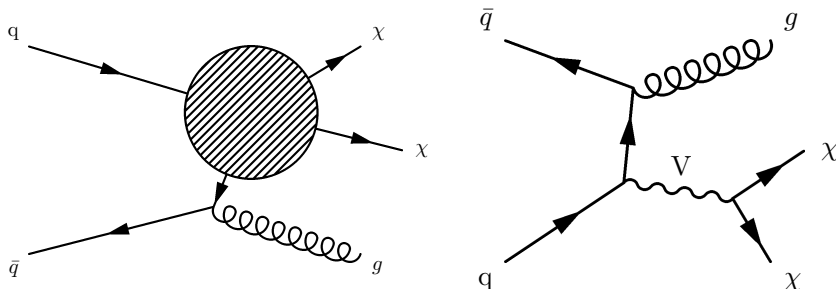
In this work, WIMPS are assumed to be Dirac fermions (half integer spin and is not its own antiparticle).

In table 1.1 the operators which are integrated out via the effective field theory and are of interest in this thesis are given.

Name	Initial state	Type	Operator
D1	qq	scalar	$\frac{m_q}{M_*^3} \bar{\chi} \chi \bar{q} q$
D5	qq	vector	$\frac{1}{M_*^2} \bar{\chi} \gamma^\mu \chi \bar{q} \gamma_\mu q$
D8	qq	axial-vector	$\frac{1}{M_*^2} \bar{\chi} \gamma^\mu \gamma^5 \chi \bar{q} \gamma_\mu \gamma^5 q$
D9	qq	tensor	$\frac{1}{M_*^2} \bar{\chi} \sigma^{\mu\nu} \chi \bar{q} \sigma_{\mu\nu} q$
D11	gg	scalar	$\frac{1}{4M_*^3} \bar{\chi} \chi \alpha_s (G_{\mu\nu}^a)^2$

Table 1.1: Table based on discussion in [13]

Where D denotes that the WIMPS are assumed to be Dirac fermions. These can all be described using figure 1.5a



(a) Effective Feynman diagram explaining the D-operators.

(b) Feynman diagram describing the vector mediator model.

Figure 1.5: Feynman diagrams describing the used signal models.

Another model which is considered is when the WIMP mass is close to the mediator mass. Then the effective theory fails and the process is assumed to be described by figure 1.5b.

1.2.6 Search for WIMPs

The search of WIMPs is based on a mono-jet analysis which is described in subsection 1.3.6. This method revolves around looking at all energy before and after

a collision and making sure energy conservation exists. If it does not, then something has happened which the detectors can not detect. If it is so that the models from subsection 1.2.5 can explain the missing energy, then a model for WIMPS has been found.

Since the search for WIMPS at the LHC is based on looking at the missing energy, not actual detection, the experiment can not establish if a WIMP is stable on a cosmological time scale and thus if it is a dark matter candidate [13]. This means that if a candidate is found, it may still not be the dark matter that is needed to explain the cosmological observations.

The different theories discussed in subsection 1.2.5 requires some process in which quarks and anti-quarks are produced. This process happens in a lot of different accelerators. The main problem is that nothing has been found low energy levels. This is why it is very interesting that the LHC is undergoing a upgrade that will allow higher energy levels, see subsection 1.3.7. With this the processes can be given higher energy and thus the produced particles can be comprised of higher mass.

1.3 Experimental overview

1.3.1 LHC

The Large hadron collider (LHC) is a particle accelerator located at CERN near Geneva in Switzerland, see figure 1.6. The accelerator was built to explore physics beyond the standard model and to make more accurate measurements of standard model physics. Before it was shut down for an upgrade in 2012 it was able to accelerate two proton beams to such a velocity that they had an energy of 4 TeV which gives a center of mass energy, $\sqrt{s} = 8$ TeV. It should be noted that the proton beam is not homogeneous, it is comprised of bunches of protons with enough spacing that bunch collisions can happen independent of each other. Apart from the energy, the ability for an accelerator to produce interactions can be calculated through the instantaneous luminosity of the LHC was $10^{34} \text{ cm}^{-2}\text{s}^{-1}$ or $10\text{nb}^{-1}\text{s}^{-1}$ where 1 barn(b)= 10^{-24} cm^2 . All values taken from [15].

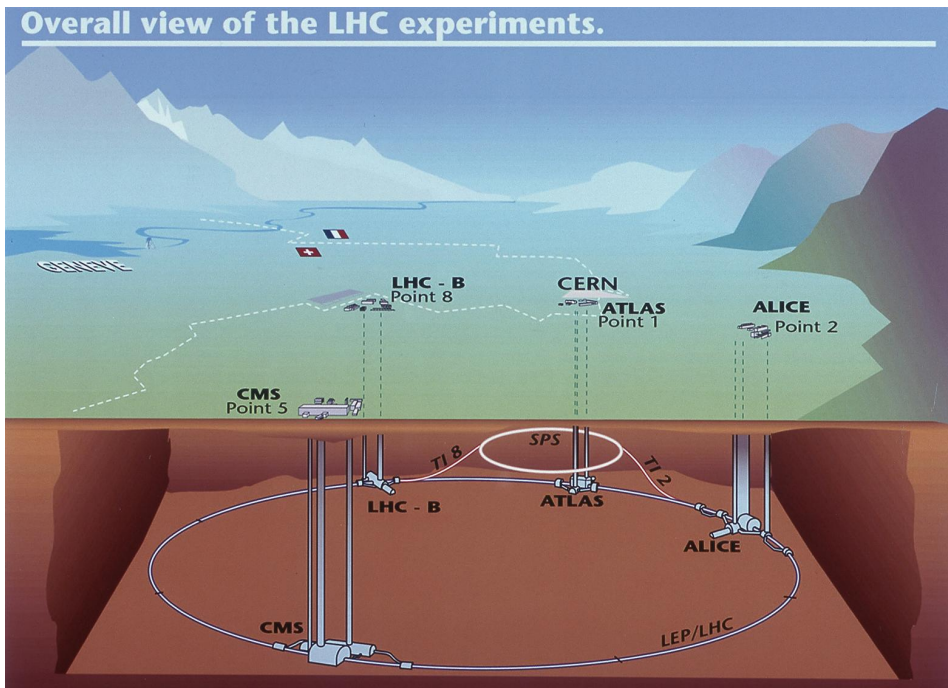


Figure 1.6: Figure showing the LHC and the different detector sites[16]

The instantaneous luminosity, often just denoted luminosity, can be defined in different ways depending on how the collision takes place. For two collinear intersecting particle beams it is defined as:

$$\mathcal{L} = \frac{f k N_1 N_2}{4\pi \sigma_x \sigma_y} \quad (1.6)$$

where N_i are the number of particles in each of the bunches, f is the frequency at which the bunches collide, k the number of colliding bunches in each beam, and σ_x (σ_y) is the horizontal (vertical) beam size at the interaction point. Since the instantaneous luminosity increases quadratically with more particles in each bunch this would be a good strategy. However aside from the difficulties to create and maintain a beam with more particles, a large N_i increases the probability for multiple collisions per bunch crossing, referred to as pile-up. Pile up will be a key aspect which is described more in subsection 1.3.5.

The expected number of events can be calculated by using the instantaneous luminosity through the following:

$$N = \sigma \int \mathcal{L} dt := \sigma \mathcal{L} \quad (1.7)$$

where \mathcal{L} is the integrated luminosity and σ is the cross section which is often measured in barn. The integrated luminosity is a measurement of total number of interactions that have occurred over time. Before the LHC was shut down this values was 20.8 fb^{-1} .

The cross section is defined through the integral of the differential cross section, as explained in subsection 1.2.1, over the whole solid angle:

$$\sigma = \oint d\Omega \frac{d\sigma}{d\Omega} \quad (1.8)$$

The cross section is therefore a measure of the effective surface area seen by the impinging particles, and as such is expressed in units of area. The cross section is proportional to the probability that an interaction will occur. It also provides a measure of the strength of the interaction between the scattered particle and the scattering center. Further details can be found in reference [17]

1.3.2 ATLAS

As seen in figure 1.6, there are several detectors at CERN. One of these is a large toroidal LHC apparatus (ATLAS) which is a general purpose detector that uses a toroid magnet. Its goal is to observe several different production and decay channels. The detector is composed of three concentric sub-detectors, the Inner detector, the Calorimeters and the Muon spectrometer [18].

The Inner detectors main job is to detect the tracks of the particles and their interaction with the material in the detector.

The Calorimeters, the electromagnetic and hadronic, are used to calculate the energy contained in the different particles (**electromagnetic get this and that, hadronic get this and that**).

The Muon spectrometer is used to detect signs of muons, which will simply pass through the other detectors without leaving a trace.

From this, it is known that neutrinos, and as assumed in this thesis WIMPS pass through all the detectors without leaving a trace.

1.3.3 Coordinate system

The coordinate system of ATLAS, seen in figure 1.7 is a right-handed coordinate system with the x-axis pointing towards the centre of the LHC tunnel, and the z-axis along the tunnel/beam (counter clockwise) seen from above. The y-axis points upward. The origin is define as the interaction point. A cylindrical coordinate system is also used for the transversal plane. (R, ϕ, Z) . For simplicity the pseudorapidity of particles from the primary vertex is defined as:

$$\eta = -\ln(\tan \frac{\theta}{2}) \quad (1.9)$$

where θ is the polar angle (xz-plane) of the particle direction measured from the positive z-axis. η is through this definition invariant under boosts in the z-direction.

It is quite common to calculate the distance between particles and jets in the (η, ϕ) plane, $d = \sqrt{(\Delta\eta)^2 + (\Delta\phi)^2}$

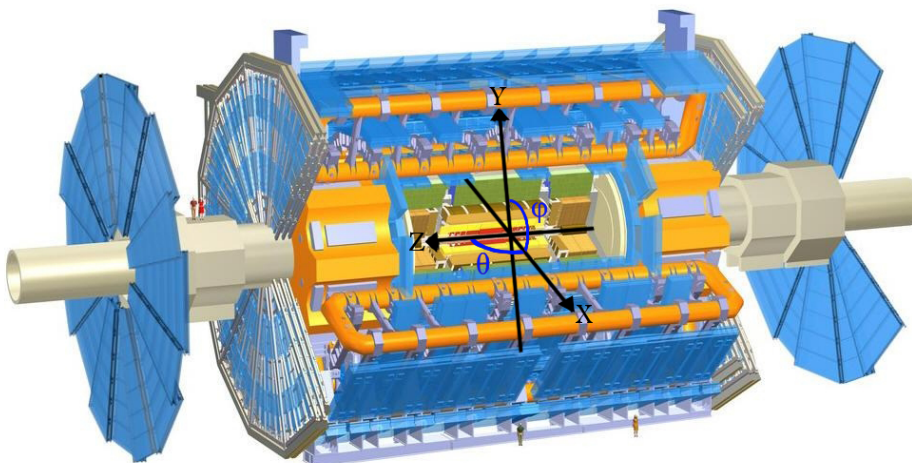


Figure 1.7: Figure showing the ATLAS detector and the definition of the orthogonal Cartesian coordinate system. Image altered from[19]

1.3.4 Reconstructing data

To be able to compare the emulated data to measurable data it is important to include effects of the detectors. This is done using so called smearing functions which try to emulate the reconstruction of data.

The reconstruction process of data [18], is based on what response is given from the detectors. It is affected by pile-up and the energy of that which is detected. The reconstruction process is not specifically used in the thesis, however the smearing functions are discussed in section 2.1.

1.3.5 Pile-up

Pile-up is defined as the average number of proton-proton collisions that occur per bunch crossing per second. It is denoted as $\langle \mu \rangle$. μ can be calculated by adjusting a Poisson distribution to fit the curve created by the number of interactions per bunch crossing at a given luminosity. When this is done μ will be the mean value of the Poisson distribution.

1.3.6 Mono-jet analysis

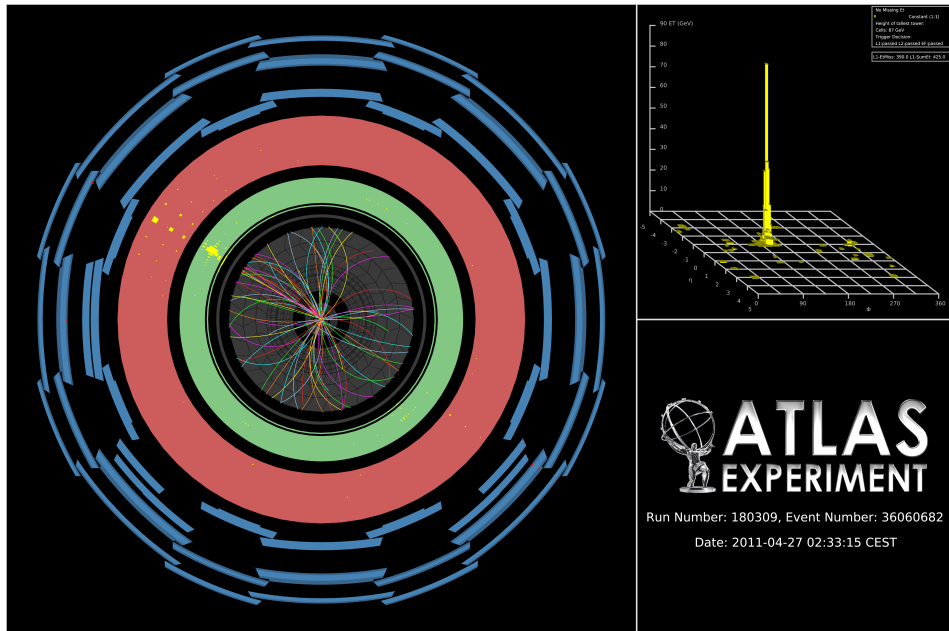


Figure 1.8: Image of a mono-jet event [20].

When measuring the transversal energy one can in some interactions find inconsistencies, such as jets that are in excess in one direction. In figure 1.8 one can see a high energetic jet which gives an excess of transversal energy in one direction after the collision. Since there is no balancing jet there must be transversal energy that is not detected, denoted E_T^{Miss} , since it was close to zero before the collision. This gives an indication that there energy to balance this that simply can not be detected. This could for instance be neutrinos or the sign of a new particle.

Jets are showers of particles that are produced at collisions. They are composed of highly energetic quarks and/or gluons. Since the gluons have self interaction, they split into even more gluons which then results in shower of particles moving in the same direction. In the final stages the quarks and gluons can combine to form larger particles. It is by measuring these end products that one can gain more information about the collision which created the jet.

There are two main concepts to the analysis, signal and background. The signal is what theoretically should be detected by a assumed process. In this thesis the different dark matter processes, from subsection 1.2.5, will constitute different signals. However to know that the missing energy is sign of the signal then one must understand all the other components that could contribute to the missing energy.

The background comprises of all the background processes that occur and that could contribute to the missing energy. By finding so called Control regions, where background process are in excess, one can model the missing energy by how many neutrinos come from the processes.

1.3.7 Phase II high luminosity upgrade

At the moment, the whole LHC is undergoing a huge upgrade program which be finalized around 2022-2023, denoted the high luminosity upgrade, or HL-upgrade. The upgrade contains of different stages, meaning that the upgrade will halt for periods so that experiments can take place. In figure 1.9 one can see the three

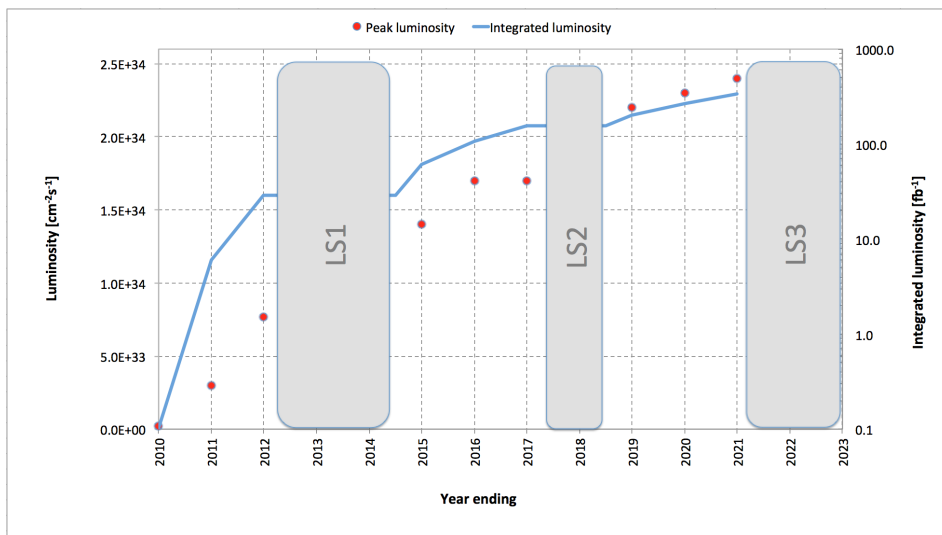


Figure 1.9: A graph showing the upgrading timetable with the instantaneous luminosity, denoted luminosity, and integrated luminosity expected in the different stages.

proposed upgrades. LS1 is denoted phase 0, LS2 phase I and LS3 phase II. LS1 is the upgrade which will take the LHC to its designed performance. LS2 will take the LHC to the ultimate designed instantaneous luminosity. LS3 which is the upgrade which is of focus in this thesis, will increase the instantaneous luminosity yet again. Though for this to happen a modification of

the whole LHC must be done, instead of just an upgrade and maintenance as before.

The following is expected for the experiments done after phase II:

Entity	Expected	Last run (2012)
Instantaneous luminosity	$\mathcal{L} \sim 50 \text{ nb}^{-1}\text{s}^{-1}$	$\mathcal{L} \sim 10 \text{ nb}^{-1}\text{s}^{-1}$
Integrated luminosity	$\mathcal{L} = 1000 - 3000 \text{ fb}^{-1}$	$\mathcal{L} = 20 \text{ fb}^{-1}$
Pile-up	$\langle \mu \rangle = 140$	$\langle \mu \rangle = 20$
Center of mass energy	$\sqrt{s} = 14 \text{ TeV}$	$\sqrt{s} = 8 \text{ TeV}$

Table 1.2: Expected running values for the Phase II HL-upgraded LHC with older values for comparison [21].

Where it should be noted that the integrated luminosity indicates the total amount of data which will be collected after the upgrade is completed before the next upgrade takes place.

1.3.8 Monte Carlo simulation

As mentioned before, in this thesis only emulated data has been used. This data is created by using a Monte Carlo simulation of the background processes and the expected signal. To do this a program called MadGraph is used.

MadGraph [22] starts with Feynman diagrams and then generates simulated events based on lots of different parameters. To create correct simulations for this analysis PYTHIA has been used.

PYTHIA [23] is a package which adds the correct description of jets and missing energy to MadGraph. PYTHIA also adds the correct description of pile-up.

The tool to access all this data and analyse it a tool called ROOT was used. ROOT is used for programming high energy physics related tools [24]

2

Validation of smearing functions

One might assume that using a Monte Carlo simulation it would be easy to model and emulate the whole process, from collision to detection and reconstruction in the upgraded LHC. It is possible, but it requires a lot of computing power. Instead one can use one simulation and a mathematical model to calculate the estimated response in the detector. This was validated and used in this thesis to be able to create the data needed for further analysis.

This was done by using a Monte Carlo simulation of a proton-proton collision and applying the official Truth to reco code, also known as the smearing functions, that was developed using previous studies [1, 25]. to simulate how the detector and the reconstruction is affected by the increased luminosity and the pile-up that comes with this.

The code uses the experimental data from the previous studies to smear the reconstructed energy and momenta, it is from this that the name smearing functions comes. The key feature of those studies were that the direction of the momenta is unaffected and that only jets and E_T^{Miss} are affected by pile-up. This was confirmed in previous studies and were thus not incorporated into the smearing functions, more in section 2.1.

2.1 Smearing functions

Put in introduction? The particles that are directly detectable in ATLAS are: electron, photon, muon, tau. Aside from this jets can be detected, and from this E_T^{Miss} can be calculated.

This means that the all detectable entities must have their own smearing functions.

E_T^{Miss} , the missing transversal energy, which was discussed in subsection 1.3.6, is calculated by knowing that there should be energy conservation in the collision. It is comprised of different parts, one from neutrinos, one from errors in the other measurements and one from (hopefully) new physics.

The jet and E_T^{Miss} are the only "parts" which are not unique particles instead they are based either on a shower of particles or the energy which is missing from the conservation of transversal energy. Thus, the pile-up dependence here must simply come from the fact that it is hard to separate the different jets and that with several different collisions occurring makes it hard to accurately measure the total energy.

The electron and photon have the same smearing since they are both detected in a similar way. Perhaps add more to the introduction about each part of the detector. or simply write that here?

The muon is special since it is detected in the muon spectrometer.

Tau is detected similarly to electron and photon.

These smearing functions are designed so that they take into account the efficiency of the different detectors, limitations as well as their dependence on pile-up. They also take into account how all this varies depending on the measured entries energy or momenta.

The terminology is that data before smearing, simulated data, is denoted as data at a truth level or truth data. Data after smearing, which is comparable to what is measured, reconstructed or reco data as discussed in subsection 1.3.4.

2.2 Validation

To validate the smearing functions a comparison with [25] was made where the standard deviation, depending on the energy or momentum value of an entity, was given, see section 2.4. To calculate this some simulated processes were needed to extract data, see table 2.1.

Data	Process
Electron	$W \rightarrow e\nu$
Muon	$W \rightarrow \mu\nu$
Tau	$W \rightarrow \tau\nu$
γ	$\gamma + \text{Jet sample}$
Jets	Jet sample
E_T^{Miss}	$Z \rightarrow \nu\nu + \text{Jet sample}$

Table 2.1: Different processes from where data has been taken. Each sample is a simulation of a physical process, the simulation names can be found in appendix A

By plotting the data for each data point before and after the smearing function, for that data point had been used, one can verify the functions. This is done looking at the reco data for a given truth energy or momentum value. Since the smearing functions take a lot of things into account the match will not be a fine line, see figure 2.3b.

By fitting a Gaussian curve to this data will then result in the mean value, and the standard deviation. The mean value is not of interest for the purposes of the thesis, though the standard deviation is since it is this which is used in the validation. The standard deviation is equivalent to RMS (Root mean square) and is also known as the resolution of the data. It will from here on be denoted RMS or σ .

This resolution is then compared to previous results, [25], and finally confirmed or demented.

To get enough and thorough statistics enough data must be available for a given truth energy or momenta and the analysis must be specific enough to only look at a minute interval around this point.

2.3 Results

As discussed above, the method was to plot the data against its smeared counterpart and through this determine the RMS, (σ) to see if it conforms to the expected values.

Since there are only slightly differences depending on pile-up these are not shown except for E_T^{Miss} and jets. Also only one energy value is shown for simplicity, though the comparison was done for different energy values.

Pile-up is fixed at 60 is nothing else is said used simply as a benchmark.

The images are, as the comparison, often divided depending on the different η values.

All results are summarized in table 2.5.

2.3.1 Electron and photon

Since these interact very similarly in the detector, their smearing functions are identical. The slice value represents at which value of unsmeared energy or momentum this smearing occurs.

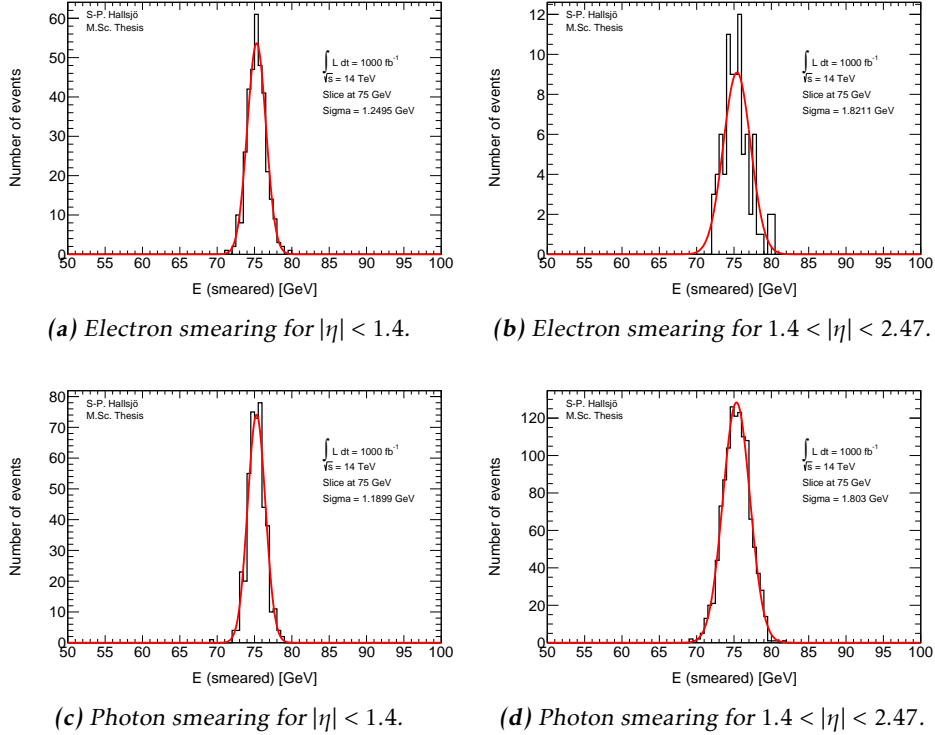


Figure 2.1: Photon and electron smearing plots.

2.3.2 Muon

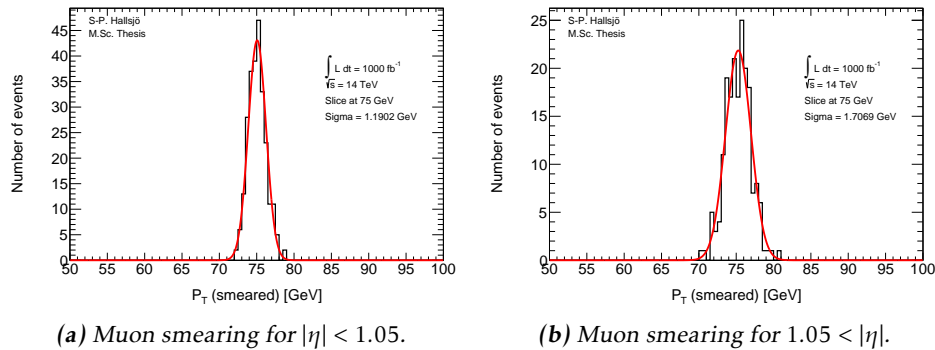


Figure 2.2: Muon smearing plots.

2.3.3 Tau

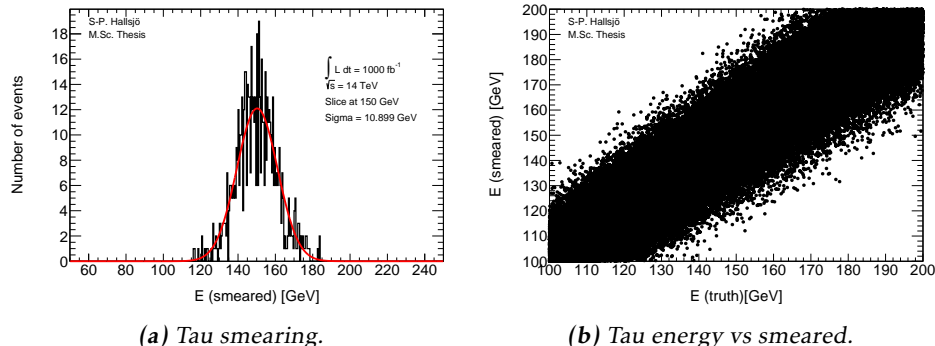


Figure 2.3: Tau smearing and energy vs smearing plot.

2.3.4 Jets

Jets as described in subsection 1.3.6, are hadronic showers. The smearing functions are divided into four different regions depending on the angle η .

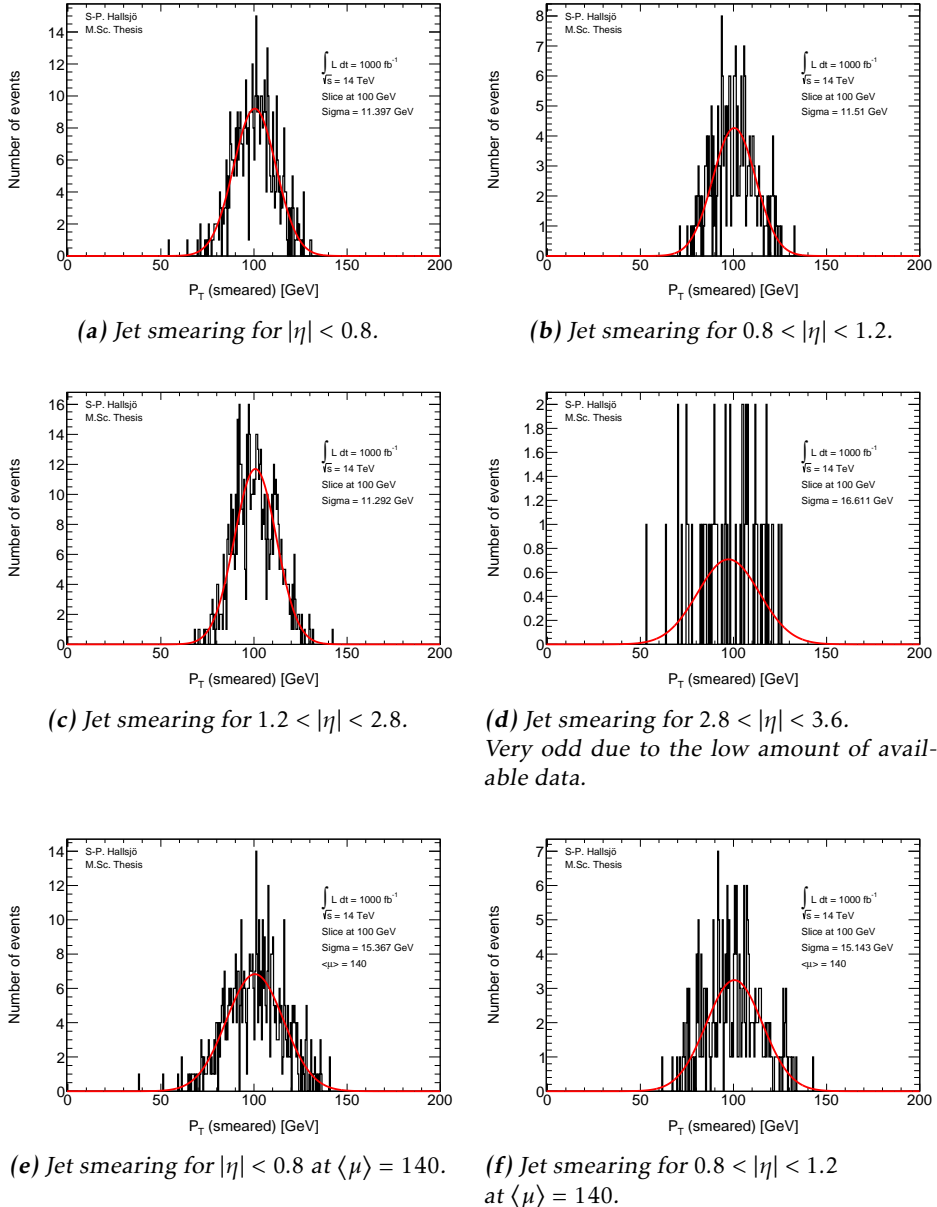


Figure 2.4: Jet smearing plots.

2.3.5 Missing Transversal Energy

These figures are given as smeared value from origin, thus at 0 it represents that the energy is unsmeared, compared to the others where the slice value represents the unsmeared.

Here the E_T^{Miss} is projected down to the x- and y-axis, since these are the transversal axes, to be smeared.

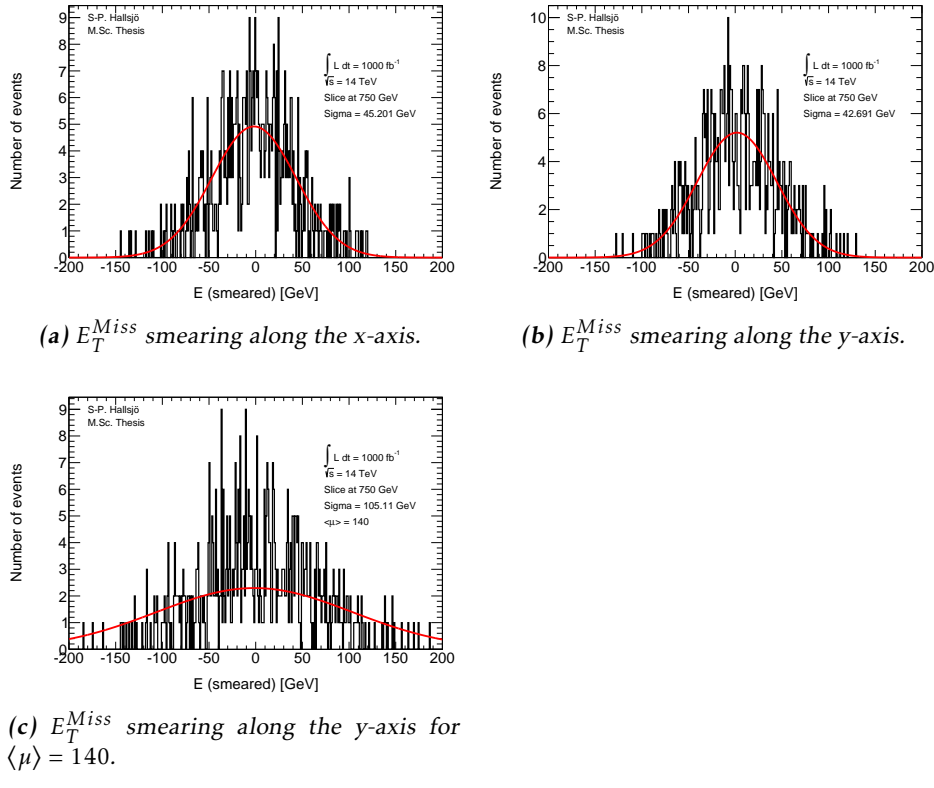


Figure 2.5: E_T^{Miss} smearing plots

2.4 Expected results

The expected response has been calculated and taken from [25].

The independence of pile-up for leptons and photons is backed up in previous research, for instance [1, 26] were the first states:

“The uncertainty due to pile-up was investigated by comparing simulated MC samples with and without pile-up and was found to be negligible”

This is also confirmed in other internal documents.

To validate the smearing code comparisons were made with [25] which gave the following formulation for the expected RMS:

Process	Absolute RMS
Electron & photon	$\sigma = 0.3 \oplus 0.1\sqrt{E(GeV)} \oplus 0.01E(GeV), \eta < 1.4$ $\sigma = 0.3 \oplus 0.15\sqrt{E(GeV)} \oplus 0.015E(GeV), 1.4 < \eta < 2.47$
Muon	$\sigma = \frac{\sigma_{id}\sigma_{ms}}{\sigma_{id} \oplus \sigma_{ms}}$ $\sigma_{id} = P_T(a_1 \oplus a_2 P_T)$ $\sigma_{ms} = P_T(\frac{b_0}{P_T} \oplus b_1 \oplus b_2 P_T)$
Tau	$\sigma = (0.03 \oplus \frac{0.76}{\sqrt{E(GeV)}})E(GeV)$
Jet	$\sigma = P_T(GeV)(\frac{N}{P_T} \oplus \frac{S}{\sqrt{P_T}} \oplus C)$
E_T^{Miss}	$\sigma = (0.4 + 0.09\sqrt{\mu})\sqrt{\sum E(GeV) + 20\mu}$

Table 2.2: Expected absolute RMS.

- For muon: All parameters are given in table 2.3.
- For tau: Fixed at 3 prong. 1 prong exists though was not used in this thesis. Where prong refers to the different amount of tracks that from which they were reconstructed.
- For jet: All parameters are given in table 2.4 where $N = a(\eta) + b(\eta)\mu$.

	a_1	a_2	b_0	b_1	b_2
$ \eta < 1.05$	0.01607	0.000307	0.24	0.02676	0.00012
$ \eta < 1.05$	0.03000	0.000307	0.00	0.03880	0.00016

Table 2.3: Parameters used in the muon smearing function take from [25].

$ \eta $	a	b	s	C
0-0.8	3.2	0.07	0.74	0.05
0.8-1.2	3.0	0.07	0.81	0.05
1.2-2.8	3.3	0.08	0.54	0.05
2.8-3.6	2.8	0.11	0.83	0.05

Table 2.4: Parameters used in the jet smearing function taken from [25].

Process	RMS [GeV]	Error in RMS	Expected RMS	Significance
Electron low η	1.24948	0.0481987	1.18427	1.35286
High η	1.8211	0.141329	1.74446	0.542334
Photon low η	1.18986	0.0400187	1.18427	0.139734
High η	1.80297	0.0374312	1.74446	1.56323
Muon low η	1.19016	0.0524938	1.49789	5.86235
High η	1.70694	0.0882606	2.18318	5.39575
Tau	10.8992	0.299761	10.3388	1.86975
Jet low η	11.3974	0.351391	11.5983	0.571586
$\langle \mu \rangle = 140$	15.3673	0.473783	15.7721	0.854499
Mid low η	11.5096	0.518872	11.9352	0.820407
$\langle \mu \rangle = 140$	15.1427	0.682649	15.9515	1.18475
Mid high η	11.2916	0.310314	10.9439	1.12021
High η	16.6112	1.52891	13.5	2.03491
E_T^{Miss} x-axis	45.2013	1.35426	48.4483	2.39762
E_T^{Miss} y-axis	42.6906	2.27904	48.4483	4.50154
$\langle \mu \rangle = 140$	105.109	12.239	87.2812	1.45667

Table 2.5: RMS values.

- Where the given RMS is still the absolute.
- The significance is the standard deviation of between the expected and calculated with respect to the error.

2.5 Discussion

2.5.1 Smearing independent on pile-up

From the validation done it was interesting to note that the smearing functions were created from previous studies, [1, 26], which had shown that leptons and photons are not affected by pile-up. This may seem incredible however it becomes quite logical when one understands how the detectors work. To be able to detect particles the detectors must detect an excess of energy which comes from a particle passing through. This should not be distorted by an increased pile-up. The amount of particles passing through will of course increase, but the detections should be unaffected as well as the recreation of the events. However with the same logic it makes sense that jets and E_T^{Miss} are quite affected since they are combined of several parts, either hadronic particles or by all the transversal missing energy.

Another interesting part is how the effect diminishes with and increasing energy. As seen above, and through the formula, for the high energies which were of interest here the effect is minimal.

2.5.2 Comparison to expected results

One of the major problems in the comparison was to get the significance of the Gaussian fit to be calculated correctly. The tool ROOT has a lot of different features which made this task somewhat difficult. Also since this is a statistical property there is a statistical fluctuation in the result.

Another was to retrieve the correct values from the paper, [25], since it was unclear if the values given were absolute or scale dependent. This has now been corrected in a new version of the paper.

2.6 Conclusion

The smearing functions work as intended within 5.8 sigma, however when using a test box and averaging the sigmas one ends up with half of this for the extreme cases, muons and E_T^{Miss} y-axis.

3

Evaluating dark matter signals

The main goal of the thesis is to investigate if certain dark matter signals can be detected after the high luminosity upgrade. One immediate worry is that the background will be large in comparison to the signal, making the signal undetectable.

The following signals models have been used: The signal models are given in appendix A along with the background. The different models were discussed in part in subsection 1.2.5 and some more in this chapter.

Each of these has been evaluated in different signal regions and the detectability has been evaluated using a statistical P-value. This process has been performed at different pile-up values.

What background existed? How was it simulated in MC? Should that be here or in appendix?

Dont mention, but good to know. Used METpt in all histograms, with the weight as in main.C and mainclass.C.

3.1 Signal to background ratio

What I am doing now, looking at what signal? What are the different background processes? What and why was the weight used?

Signals should be explained somewhat in the introduction.

Look at presentation, is it worth bringing up the first signal regions when the data has already been filtered? Should that be here?

3.1.1 Selection criteria

What criteria were used and more importantly why? It is quite important that you can explain why this was used.

For different purposes different selection criteria or regions are used. These are a set of criteria specified to enhance the area of interest. For instance, if simulating a specific signal one wants to find as many ways as possible to diminish the background. This so that when searching experimentally, the signal will be easier to detect.

These can be quite general cuts, there are only some things to take into consideration.

- If experimental, what limitations are set by the detectors? Are there some criteria already?
- If simulated, is there some criteria set in the generator?
- Are there criteria which must be set since there is too much uncertainty in the data? or a large effect of pile up?

3.1.2 Verifying background data

To verify that the background data was correct it was compared with [27], in which the luminosity is 10 fb^{-1} and thus the expected values from the paper scaled up with a factor 100. **Also, somewhat unexpectedly is that the difference in center of mass energy required the cross-sections to be much lowered than compared with the upgrade.** The signal region used in the article were the following:

Selection Criteria		
Jet veto, require no more than 2 jets with $p_T > 30 \text{ GeV}$ and $ \eta < 4.5$		
Lepton veto, no electron or muon		
Leading jet with $ \eta < 2.0$ and $\Delta\phi(\text{jet}, E_T^{\text{Miss}}) > 0.5$ (second-leading jet)		
signal region	SR3p	SR4p
minimum leading jet p_T (GeV)	350	500
minimum E_T^{Miss} (GeV)	350	500

Table 3.1: The signal regions

The article has several different signal regions, the difference is the last item, unfortunately since the simulated events are already filtered before the analysis only one of the regions could be used.

NEW WITH 350 as SR3 and 500 as SR4 and expected (Scaled to 1000 fb^{-1}) thus scaled a factor 100 since luminosity is only a measurement of the amount of data and does not change anything physical.

Process	SR3p	Expected SR3p	SR4p	Expected SR4p
$Z \rightarrow \nu\nu$	140298	152000	25250.3	27000
$W \rightarrow \tau\nu$	40700.8	37000	5861.74	3900
$W \rightarrow e\nu$	11229	11200	1506.58	1600
$W \rightarrow \mu\nu$	13727.1	15800	1872.32	4200
Total background	205955	218000	34491	36700

Table 3.2: Comparison of the simulated and expected events from [27].

In table 3.2 a comparison has been made. It can be seen that the simulated events and expected events coincide on all accounts apart from $W \rightarrow \tau\nu$, $W \rightarrow \mu\nu$ and thus the total as well. **This can be explained by better separation of μ, τ and missing energy.** Tau can not be reconstructed as jets in the code, they can in reality!

3.1.3 Figures of merit

P-value, info from Majas phd thesis. Is there a source? Should there be a figure?

To be able to evaluate different signal regions and different signal models, a figure of merit p is used. The value p is the probability for an assumed hypothesis to be correct, thus a good signal region will yield a low value. The assumed hypothesis is that the background and its fluctuations is measured over the signal plus background.

Assuming the expected number of background events are $B \pm \sigma_B$ where σ_B is the quadratic sum of the statistical error from Monte Carlo, the statistical error from the control region and the systematic errors. The expected number of signals is S , assumed without fluctuation.

If no uncertainty in B or S is assumed, then the number of expected events, N , in the signal region should follow a Poisson distribution as such:

$$P(N|S+B) = \frac{e^{-(S+B)}(S+B)^N}{N!} \quad (3.1)$$

However since there is an uncertainty in the background, the probability distribution $P(N|S+B)$ must be convoluted with a Gaussian function:

$$G(N_B|B, \sigma_B) = \frac{1}{\sigma_B \sqrt{2\pi}} e^{-\frac{(N_B-B)^2}{2\sigma_B^2}} \quad (3.2)$$

where N_B is the expected number of background events. The convolution is done

using N_B as N resulting in the total probability density function:

$$\begin{aligned} F(N|S+B, \sigma_B) &= P(N|S+N_B)*G(N_B|B, \sigma_B) = \\ &= \int_{-\infty}^{\infty} P(N|N_B - (S + B))G(N_B|B, \sigma_B)dN_B \end{aligned} \quad (3.3)$$

This leads to the probability of the signal plus background fluctuation to B events being obtained by summing the probability function from $N=0$ to $N=B$.

$$p = \sum_{i=0}^B \int_{-\infty}^{\infty} P(i|N_B-(S+B))G(N_B|B, \sigma_B)dN_B \quad (3.4)$$

3.1.4 D5 operators

Discuss M^* , and the difference in mDM. From presentation given, 3-4 April.

Was discussed in part in subsection 1.2.5

As described in the introduction [reference?](#), one of the signals is modelled using the D5 operator. In this thesis two different scenarios were used, one at a dark matter mass of 50 GeV and one at 400 GeV.

3.1.5 Light vector mediator models

Discuss M_m , width, and the difference in mDM. From presentation given, 3-4 April.

Was discussed in part in subsection 1.2.5

As described in the introduction [reference?](#), the other signal model is a vector mediator model. The data available is: two different widths $M/3$ and $M/8\pi$. $M_!?$ two different mDM, 50 GeV and 400 GeV and finally a variety of mediator masses.

3.1.6 Susy models?

3.2 Other selection criteria and observables

New signal regions.

3.3 Mitigating the effect of the high luminosity

Something pile-up Something as seen in validation of... the effect is quite minute for high energy values and does not at all affect leptons or photons. Mention that the effect is on a trigger level, that the lowest SR will be lost.

Even though this was envisioned as the primary focus of the thesis, it was shown that the effect of pile-up is minute for these high signal regions. Thus the focus

Selection Criteria

Jet veto, require no more than 2 jets with $p_T > 30\text{GeV}$ and $|\eta| < 4.5$

Lepton veto, no electron or muon

Leading jet with $|\eta| < 2.0$ and $\Delta\phi(\text{jet}, E_T^{\text{Miss}}) > 0.5$ (second-leading jet)

signal region	SR0	SR1	SR2	SR3	SR4
minimum leading jet p_T (GeV)	120	350	600	800	1000
minimum E_T^{Miss} (GeV)	120	350	600	800	1000
signal region	SR0	SRa	SRb	SRc	SRd
minimum leading jet p_T (GeV)	350	350	350	350	350
minimum E_T^{Miss} (GeV)	120	350	600	800	1000

Table 3.3: The new signal regions

was shifted to perform a more in-depth mono-jet analysis of different DM signal models.

3.4 Results

3.4.1 Limit on M^*

The mass suppression scale. Give at 1000fb^{-1} . And for the different signal regions. **ASK CHRISTOPHE FOR A GOOD EXPLANATION OF M^* and why there can be limits!**

For the new signal regions: **Include a table of the limits for truth and Reco.**

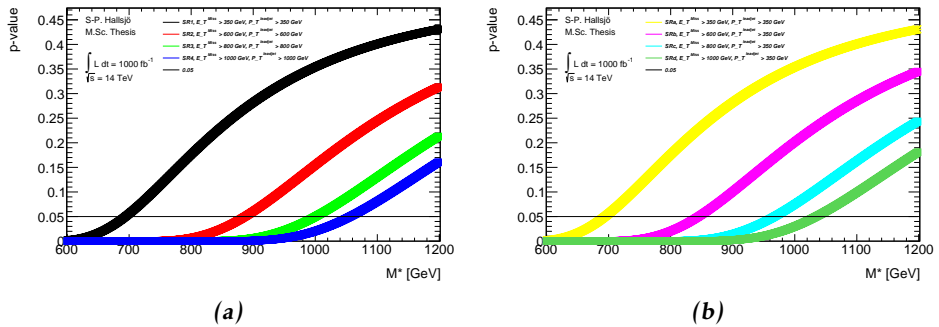


Figure 3.1: On a truth level.

3.4.2 Effect of pile-up on M^*

Hardly any effect. 10 % or in that vicinity.

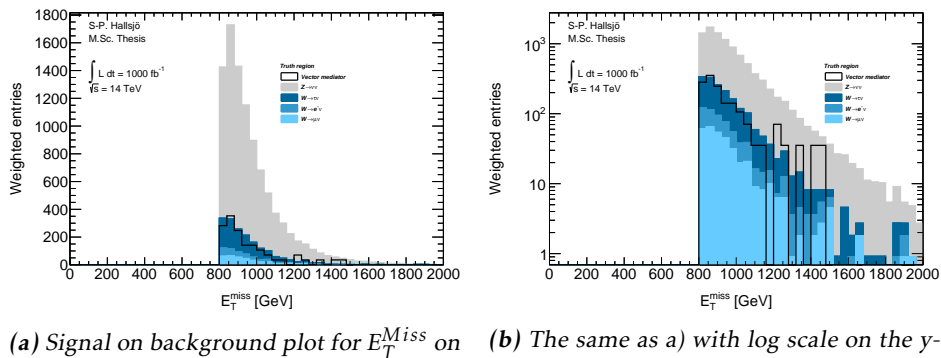
3.4.3 Previous results

Valerios paper for instance. Preliminary note that much better results for 1000fb-1 and 14TeV.

The whole discussion with Steven and David.

3.4.4 Limit on mediator mass

Are there previous results? Signal vs background plot in normal and log scale for one of the vector mediator models, to be able to evaluate all the different models the so called p-value was used in different signal regions. Below are two figures showing one of the vector mediator models in SR3.



(a) Signal on background plot for E_T^{Miss} on reco level in SR3. (b) The same as a) with log scale on the y-axis

Figure 3.2: Signal on background plot to illustrate the a general plot.

To set a limit on the mediator mass the p-value was calculated in different signal regions for the different signal models with different mediator mass. This resulted in the following plot:

3.4.5 Effect of pile-up on mediator mass

Check the different cases for reco and truth to see what happens.

3.5 Discussion

3.6 Conclusion

4

Results and Conclusions

4.1 Validation of smearing functions

Have some discussion.

Result they appear to work as expected, the reference paper was a bit unclear, I leave my writing as a better reference.

4.2 Signal to background ratio

4.2.1 Limit on M^*

4.2.2 Limit on mediator mass

4.3 Other selection criteria and observables

4.3.1 Limit on M^*

4.3.2 Limit on mediator mass

4.4 Mitigating the effect of the high luminosity

4.5 Recommendations to mitigate the effect of the high luminosity

Keep to a higher energy region, or signal region.

4.6 Suggestions for future research

With more time, search for new signal regions, the only solution now for the HL is to go up in energy. Since none of the other parameters (eta,phi etc) seem to be altered these can not be used. Is there something that has been overlooked?

Test the effect of pile-up for lower signal regions? See if the effect is as great as predicted.

Explore other theoretical models for dark matter, other d operators etc. Models that are based on Supersymmetry and not just effective theories.

Sätt av ett kort kapitel sist i rapporten till att avrunda och föreslå räkningar för framtida utveckling av arbetet.

Saving as reference. test citing as: Here we cite Duck [28] [28].

If the above works, remember to edit myreferences.

Appendix

A

Datasets

A.1 Background processes

A.1.1 Validation

For the validation the following datasets were used, with a filter at generator level at 450GeV for lead jet and MET.

mc12.157539.sherpa_ct10_znunupt280d4pd.v03 mc12.157534.sherpa_ct10_wenupt200d4pd.v03

mc12.157535.sherpa_ct10_wmunupt200d4pd.v03

mc12.157536.sherpa_ct10_wtaunupt200d4pd.v03

mc12.129160.pythia8_au2cteq6l1_perf_jf17d4pd.v03

mc12.129160.pythia8_au2cteq6l1_perf_jf17d4pd.v04

mc12.129170.pythia8_au2cteq6l1_gammajet_dp17d4pd.v04

They should be read as such: Monte Carlo version, dataset number, generator, ? name.

A.1.2 Background to signals

The same as the above though now with the filter as indicated by their name. The second znunu sample has been generated with and center of mass energy at 8 TeV.

mc12.157539.sherpa_ct10_znunupt280d4pd.v05

mc12.157539.8tev_sherpa_ct10_znunupt280d4pd.v05

mc12.157536.sherpa_ct10_wtaunupt200d4pd.v05

mc12.157534.sherpa_ct10_wenupt200d4pd.v05

mc12.157535.sherpa_ct10_wmunupt200d4pd.v05

A.2 D5 signal processes

```

mc12.188408.madgraphpythia_auet2bcteq6l1_d5_dm50_ms10000_
qcut200d4pd.v06
mc12.188409.madgraphpythia_auet2bcteq6l1_d5_dm50_ms10000_
qcut400d4pd.v06
mc12.188410.madgraphpythia_auet2bcteq6l1_d5_dm50_ms10000_
qcut600d4pd.v06

mc12.188411.madgraphpythia_auet2bcteq6l1_d5_dm400_ms10000_
qcut200d4pd.v06
mc12.188412.madgraphpythia_auet2bcteq6l1_d5_dm400_ms10000_
qcut400d4pd.v06
mc12.188413.madgraphpythia_auet2bcteq6l1_d5_dm400_ms10000_
qcut600d4pd.v06

```

All signals should be read as such: Monte Carlo version, dataset number, generator, ?, name of operator, dark matter mass, default mass suppression scale, qcut part. As discussed in [reference](#)

qcut means that the original data has been split into different parts depending on the value of the lead jet pt.

A.3 Light vector mediator processes

```

mc12.188414.madgraphpythia_auet2bcteq6l1_dmv_dm50_mm100_w3_
qcut200d4pd.v06
mc12.188422.madgraphpythia_auet2bcteq6l1_dmv_dm50_mm100_w3_
qcut400d4pd.v06
mc12.188430.madgraphpythia_auet2bcteq6l1_dmv_dm50_mm100_w3_
qcut600d4pd.v06

mc12.188415.madgraphpythia_auet2bcteq6l1_dmv_dm50_mm300_w3_
qcut200d4pd.v06
mc12.188423.madgraphpythia_auet2bcteq6l1_dmv_dm50_mm300_w3_
qcut400d4pd.v06
mc12.188431.madgraphpythia_auet2bcteq6l1_dmv_dm50_mm300_w3_
qcut600d4pd.v06

mc12.188416.madgraphpythia_auet2bcteq6l1_dmv_dm50_mm500_w3_
qcut200d4pd.v06
mc12.188424.madgraphpythia_auet2bcteq6l1_dmv_dm50_mm500_w3_
qcut400d4pd.v06
mc12.188432.madgraphpythia_auet2bcteq6l1_dmv_dm50_mm500_w3_
qcut600d4pd.v06

mc12.188417.madgraphpythia_auet2bcteq6l1_dmv_dm50_mm1000_w3_
qcut200d4pd.v06
mc12.188425.madgraphpythia_auet2bcteq6l1_dmv_dm50_mm1000_w3_

```

```
qcut400d4pd.v06
mc12.188433.madgraphpythia_auet2bcteq6l1_dmv_dm50_mm1000_w3_
qcut600d4pd.v06

mc12.188418.madgraphpythia_auet2bcteq6l1_dmv_dm50_mm3000_w3_
qcut200d4pd.v06
mc12.188426.madgraphpythia_auet2bcteq6l1_dmv_dm50_mm3000_w3_
qcut400d4pd.v06
mc12.188434.madgraphpythia_auet2bcteq6l1_dmv_dm50_mm3000_w3_
qcut600d4pd.v06

mc12.188419.madgraphpythia_auet2bcteq6l1_dmv_dm50_mm6000_w3_
qcut200d4pd.v06
mc12.188427.madgraphpythia_auet2bcteq6l1_dmv_dm50_mm6000_w3_
qcut400d4pd.v06
mc12.188435.madgraphpythia_auet2bcteq6l1_dmv_dm50_mm6000_w3_
qcut600d4pd.v06

mc12.188420.madgraphpythia_auet2bcteq6l1_dmv_dm50_mm10000_w3_
qcut200d4pd.v06
mc12.188428.madgraphpythia_auet2bcteq6l1_dmv_dm50_mm10000_w3_
qcut400d4pd.v06
mc12.188436.madgraphpythia_auet2bcteq6l1_dmv_dm50_mm10000_w3_
qcut600d4pd.v06

mc12.188421.madgraphpythia_auet2bcteq6l1_dmv_dm50_mm15000_w3_
qcut200d4pd.v06
mc12.188429.madgraphpythia_auet2bcteq6l1_dmv_dm50_mm15000_w3_
qcut400d4pd.v06
mc12.188437.madgraphpythia_auet2bcteq6l1_dmv_dm50_mm15000_w3_
qcut600d4pd.v06

mc12.188438.madgraphpythia_auet2bcteq6l1_dmv_dm50_mm100_w8pi_
qcut200d4pd.v06
mc12.188446.madgraphpythia_auet2bcteq6l1_dmv_dm50_mm100_w8pi_
qcut400d4pd.v06
mc12.188454.madgraphpythia_auet2bcteq6l1_dmv_dm50_mm100_w8pi_
qcut600d4pd.v06

mc12.188439.madgraphpythia_auet2bcteq6l1_dmv_dm50_mm300_w8pi_
qcut200d4pd.v06
mc12.188447.madgraphpythia_auet2bcteq6l1_dmv_dm50_mm300_w8pi_
qcut400d4pd.v06
mc12.188455.madgraphpythia_auet2bcteq6l1_dmv_dm50_mm300_w8pi_
qcut600d4pd.v06

mc12.188440.madgraphpythia_auet2bcteq6l1_dmv_dm50_mm500_w8pi_
qcut200d4pd.v06
mc12.188448.madgraphpythia_auet2bcteq6l1_dmv_dm50_mm500_w8pi_
```

qcut400d4pd.v06
mc12.188456.madgraphpythia_auet2bcteq6l1_dmv_dm50_mm500_w8pi_qcut600d4pd.v06

mc12.188441.madgraphpythia_auet2bcteq6l1_dmv_dm50_mm1000_w8pi_qcut200d4pd.v06
mc12.188449.madgraphpythia_auet2bcteq6l1_dmv_dm50_mm1000_w8pi_qcut400d4pd.v06
mc12.188457.madgraphpythia_auet2bcteq6l1_dmv_dm50_mm1000_w8pi_qcut600d4pd.v06

mc12.188442.madgraphpythia_auet2bcteq6l1_dmv_dm50_mm3000_w8pi_qcut200d4pd.v06
mc12.188450.madgraphpythia_auet2bcteq6l1_dmv_dm50_mm3000_w8pi_qcut400d4pd.v06
mc12.188458.madgraphpythia_auet2bcteq6l1_dmv_dm50_mm3000_w8pi_qcut600d4pd.v06

mc12.188444.madgraphpythia_auet2bcteq6l1_dmv_dm50_mm10000_w8pi_qcut200d4pd.v06
mc12.188452.madgraphpythia_auet2bcteq6l1_dmv_dm50_mm10000_w8pi_qcut400d4pd.v06
mc12.188460.madgraphpythia_auet2bcteq6l1_dmv_dm50_mm10000_w8pi_qcut600d4pd.v06

mc12.188445.madgraphpythia_auet2bcteq6l1_dmv_dm50_mm15000_w8pi_qcut200d4pd.v06
mc12.188453.madgraphpythia_auet2bcteq6l1_dmv_dm50_mm15000_w8pi_qcut400d4pd.v06
mc12.188461.madgraphpythia_auet2bcteq6l1_dmv_dm50_mm15000_w8pi_qcut600d4pd.v06

mc12.188462.madgraphpythia_auet2bcteq6l1_dmv_dm400_mm500_w3_qcut200d4pd.v06
mc12.188468.madgraphpythia_auet2bcteq6l1_dmv_dm400_mm500_w3_qcut400d4pd.v06
mc12.188474.madgraphpythia_auet2bcteq6l1_dmv_dm400_mm500_w3_qcut600d4pd.v06

mc12.188463.madgraphpythia_auet2bcteq6l1_dmv_dm400_mm1000_w3_qcut200d4pd.v06
mc12.188469.madgraphpythia_auet2bcteq6l1_dmv_dm400_mm1000_w3_qcut400d4pd.v06
mc12.188475.madgraphpythia_auet2bcteq6l1_dmv_dm400_mm1000_w3_qcut600d4pd.v06

mc12.188464.madgraphpythia_auet2bcteq6l1_dmv_dm400_mm3000_w3_qcut200d4pd.v06
mc12.188470.madgraphpythia_auet2bcteq6l1_dmv_dm400_mm3000_w3_

```
qcut400d4pd.v06
mc12.188476.madgraphpythia_auet2bcteq6l1_dmv_dm400_mm3000_w3_
qcut600d4pd.v06

mc12.188465.madgraphpythia_auet2bcteq6l1_dmv_dm400_mm6000_w3_
qcut200d4pd.v06
mc12.188471.madgraphpythia_auet2bcteq6l1_dmv_dm400_mm6000_w3_
qcut400d4pd.v06
mc12.188477.madgraphpythia_auet2bcteq6l1_dmv_dm400_mm6000_w3_
qcut600d4pd.v06

mc12.188466.madgraphpythia_auet2bcteq6l1_dmv_dm400_mm10000_w3_
qcut200d4pd.v06
mc12.188472.madgraphpythia_auet2bcteq6l1_dmv_dm400_mm10000_w3_
qcut400d4pd.v06
mc12.188478.madgraphpythia_auet2bcteq6l1_dmv_dm400_mm10000_w3_
qcut600d4pd.v06

mc12.188467.madgraphpythia_auet2bcteq6l1_dmv_dm400_mm15000_w3_
qcut200d4pd.v06
mc12.188473.madgraphpythia_auet2bcteq6l1_dmv_dm400_mm15000_w3_
qcut400d4pd.v06
mc12.188479.madgraphpythia_auet2bcteq6l1_dmv_dm400_mm15000_w3_
qcut600d4pd.v06

mc12.188480.madgraphpythia_auet2bcteq6l1_dmv_dm400_mm500_w8pi_
qcut200d4pd.v06
mc12.188486.madgraphpythia_auet2bcteq6l1_dmv_dm400_mm500_w8pi_
qcut400d4pd.v06
mc12.188492.madgraphpythia_auet2bcteq6l1_dmv_dm400_mm500_w8pi_
qcut600d4pd.v06

mc12.188481.madgraphpythia_auet2bcteq6l1_dmv_dm400_mm1000_w8pi_
qcut200d4pd.v06
mc12.188487.madgraphpythia_auet2bcteq6l1_dmv_dm400_mm1000_w8pi_
qcut400d4pd.v06
mc12.188493.madgraphpythia_auet2bcteq6l1_dmv_dm400_mm1000_w8pi_
qcut600d4pd.v06

mc12.188482.madgraphpythia_auet2bcteq6l1_dmv_dm400_mm3000_w8pi_
qcut200d4pd.v06
mc12.188488.madgraphpythia_auet2bcteq6l1_dmv_dm400_mm3000_w8pi_
qcut400d4pd.v06
mc12.188494.madgraphpythia_auet2bcteq6l1_dmv_dm400_mm3000_w8pi_
qcut600d4pd.v06

mc12.188483.madgraphpythia_auet2bcteq6l1_dmv_dm400_mm6000_w8pi_
qcut200d4pd.v06
mc12.188489.madgraphpythia_auet2bcteq6l1_dmv_dm400_mm6000_w8pi_
```

qcut400d4pd.v06
mc12.188495.madgraphpythia_auet2bcteq6l1_dmv_dm400_mm6000_w8pi_qcut600d4pd.v06

mc12.188484.madgraphpythia_auet2bcteq6l1_dmv_dm400_mm10000_w8pi_qcut200d4pd.v06
mc12.188490.madgraphpythia_auet2bcteq6l1_dmv_dm400_mm10000_w8pi_qcut400d4pd.v06
mc12.188496.madgraphpythia_auet2bcteq6l1_dmv_dm400_mm10000_w8pi_qcut600d4pd.v06

mc12.188485.madgraphpythia_auet2bcteq6l1_dmv_dm400_mm15000_w8pi_qcut200d4pd.v06
mc12.188491.madgraphpythia_auet2bcteq6l1_dmv_dm400_mm15000_w8pi_qcut400d4pd.v06
mc12.188497.madgraphpythia_auet2bcteq6l1_dmv_dm400_mm15000_w8pi_qcut600d4pd.v06

Bibliography

- [1] Collaboration ATLAS. Letter of Intent for the Phase-II Upgrade of the ATLAS Experiment. Dec 2012. URL <https://cds.cern.ch/record/1502664/>. Cited on pages 1, 17, 25, and 27.
- [2] B.H. Bransden and C.J. Joachain. *Quantum mechanics*. Pearson Education, second edition, 2000. Cited on page 3.
- [3] Sven-Patrik Hallsjö. Covering the sphere with noncontextuality inequalities. Bachelor's thesis, Linköping University, The Institute of Technology, 2013. URL [http://urn.kb.se/resolve?urn=urn:nbn:se:liu:diva-103663](http://urn.kb.se/resolve?urn=urn:nbn:se:liu.diva-103663). Cited on page 3.
- [4] A. Zee. *Quantum Field Theory in a Nutshell*. Princeton University Press, illustrated edition edition, March 2003. ISBN 0691010196. Cited on pages 3, 6, and 7.
- [5] Herbert Goldstein, Charles P. Poole, and John L. Safko. *Classical Mechanics (3rd Edition)*. Addison-Wesley, 3 edition, June 2001. ISBN 0201657023. Cited on page 3.
- [6] W. E. Burcham and M. Jobes. *Nuclear and Particle Physics*. Pearson education, second edition, 1995. Cited on page 4.
- [7] The ATLAS Collaboration. Observation of a new particle in the search for the Standard Model Higgs boson with the ATLAS detector at the LHC. *Phys. Lett. B*, 716(arXiv:1207.7214). CERN-PH-EP-2012-218):1–29. 39 p, Aug 2012. Cited on page 4.
- [8] Standard model of elementary particles. http://en.wikipedia.org/wiki/File:Standard_Model_of_Elementary_Particles.svg, 2014. Accessed: 2014-03-24. Cited on page 4.
- [9] G. Jungman, M. Kamionkowski, and K. Griest. Supersymmetric dark matter. *Physics Reports*, 267:195–373, March 1996. doi: 10.1016/0370-1573(95)00058-5. Cited on pages 4, 5, and 6.

- [10] NASA. NASA's solar system exploration: the planets: orbits and physical characteristics. <https://solarsystem.nasa.gov/planets/charchart.cfm>, 2014. Accessed: 2014-03-21. Cited on page 6.
- [11] T. S. van Albada, J. N. Bahcall, K. Begeman, and R. Sancisi. Distribution of dark matter in the spiral galaxy NGC 3198. *Astrophysical Journal*, 295: 305–313, August 1985. doi: 10.1086/163375. Cited on page 6.
- [12] Jessica Goodman, Masahiro Ibe, Arvind Rajaraman, William Shepherd, Tim M.P. Tait, et al. Constraints on Light Majorana dark Matter from Colliders. *Phys.Lett.*, B695:185–188, 2011. doi: 10.1016/j.physletb.2010.11.009. Cited on pages 5 and 7.
- [13] ATLAS Collaboration. Search for dark matter candidates and large extra dimensions in events with a jet and missing transverse momentum with the atlas detector. *J. High Energy Phys.*, 04(arXiv:1210.4491. CERN-PH-EP-2012-210):075. 58 p, October 2012. URL <http://cds.cern.ch/record/1485031>. Cited on pages 5, 8, and 9.
- [14] J. Goodman, M. Ibe, A. Rajaraman, W. Shepherd, T. M. P. Tait, and H.-B. Yu. Constraints on dark matter from colliders. *Phys.Rev.D82:116010,2010*, 82(11):116010, December 2010. doi: 10.1103/PhysRevD.82.116010. Cited on page 7.
- [15] ATLAS. Atlas luminosity public results. <https://twiki.cern.ch/twiki/bin/view/AtlasPublic/LuminosityPublicResults>, 2013. Accessed: 2014-03-06. Cited on page 10.
- [16] AC Team. The four main LHC experiments, Jun 1999. URL <http://cds.cern.ch/record/40525>. Cited on page 10.
- [17] Werner Herr and B Muratori. Concept of luminosity. 2006. URL <http://cds.cern.ch/record/941318/>. Cited on page 11.
- [18] The ATLAS Collaboration. The atlas experiment at the cern large hadron collider. *Journal of Instrumentation*, 3(08):S08003. 437 p, 2008. URL <https://cdsweb.cern.ch/record/1129811/>. Cited on pages 11 and 12.
- [19] Joao Pequenao. Computer generated image of the whole ATLAS detector, Mar 2008. URL <http://cds.cern.ch/record/1095924>. Cited on page 12.
- [20] ATLAS Collaboration. Event display for one of the monojet candidates in the data. The event has a jet with $\text{pt} = 602 \text{ GeV}$ at $\eta = -1$ and $\phi = 2.6$, $\text{MET} = 523 \text{ GeV}$, and no additional jet with $\text{pt}_{\text{jet}} > 30 \text{ GeV}$ in the final state.. https://atlas.web.cern.ch/Atlas/GROUPS/PHYSICS/CONFNOTES/ATLAS-CONF-2011-096/fig_08.png, 2011. Accessed: 2014-03-28. Cited on page 13.
- [21] ATLAS Collaboration. Physics at a High-Luminosity LHC with ATLAS. Jul

2013. URL <https://cds.cern.ch/record/1564937>. Cited on page 15.
- [22] J. Alwall, M. Herquet, F. Maltoni, O. Mattelaer, and T. Stelzer. MadGraph 5: going beyond. *Journal of High Energy Physics*, 6:128, June 2011. doi: 10.1007/JHEP06(2011)128. Cited on page 15.
- [23] Torbjörn Sjöstrand, Stephen Mrenna, and Peter Skands. A brief introduction to {PYTHIA} 8.1. *Computer Physics Communications*, 178(11):852 – 867, 2008. ISSN 0010-4655. doi: <http://dx.doi.org/10.1016/j.cpc.2008.01.036>. URL <http://www.sciencedirect.com/science/article/pii/S0010465508000441>. Cited on page 15.
- [24] The ROOT Team. Root. <http://root.cern.ch/drupal/>, 2014. Accessed: 2014-03-28. Cited on page 15.
- [25] ATLAS Collaboration. Performance assumptions for an upgraded ATLAS detector at a High-Luminosity LHC. Mar 2013. URL <https://cds.cern.ch/record/1527529/>. Cited on pages 17, 19, 25, 26, and 27.
- [26] ATLAS Collaboration. Electron performance measurements with the ATLAS detector using the 2010 LHC proton-proton collision data. *Eur. Phys. J. C*, 72(arXiv:1110.3174. CERN-PH-EP-2011-117):1909. 45 p, Oct 2011. Comments: 33 pages plus author list (45 pages total), 24 figures, 12 tables, submitted to Eur. Phys. J. C. Cited on pages 25 and 27.
- [27] ATLAS Collaboration. Search for New Phenomena in Monojet plus Missing Transverse Momentum Final States using 10fb⁻¹ of pp Collisions at sqrt(s)=8 TeV with the ATLAS detector at the LHC. Nov 2012. URL <http://cds.cern.ch/record/1493486/>. Cited on pages 30 and 31.
- [28] Donald Duck. The history of automatic control. *Duckburg Journal of Science*, 106(3):345–401, 2005. Cited on page 36.





Upphovsrätt

Detta dokument hålls tillgängligt på Internet — eller dess framtida ersättare — under 25 år från publiceringsdatum under förutsättning att inga extraordinära omständigheter uppstår.

Tillgång till dokumentet innebär tillstånd för var och en att läsa, ladda ner, skriva ut enstaka kopior för enskilt bruk och att använda det oförändrat för icke-kommersiell forskning och för undervisning. Överföring av upphovsrätten vid en senare tidpunkt kan inte upphäva detta tillstånd. All annan användning av dokumentet kräver upphovsmannens medgivande. För att garantera äktheten, säkerheten och tillgängligheten finns det lösningar av teknisk och administrativ art.

Upphovsmannens ideella rätt innehåller rätt att bli nämnd som upphovsman i den omfattning som god sed kräver vid användning av dokumentet på ovan beskrivna sätt samt skydd mot att dokumentet ändras eller presenteras i sådan form eller i sådant sammanhang som är kränkande för upphovsmannens litterära eller konstnärliga anseende eller egenart.

För ytterligare information om Linköping University Electronic Press se förlagets hemsida <http://www.ep.liu.se/>

Copyright

The publishers will keep this document online on the Internet — or its possible replacement — for a period of 25 years from the date of publication barring exceptional circumstances.

The online availability of the document implies a permanent permission for anyone to read, to download, to print out single copies for his/her own use and to use it unchanged for any non-commercial research and educational purpose. Subsequent transfers of copyright cannot revoke this permission. All other uses of the document are conditional on the consent of the copyright owner. The publisher has taken technical and administrative measures to assure authenticity, security and accessibility.

According to intellectual property law the author has the right to be mentioned when his/her work is accessed as described above and to be protected against infringement.

For additional information about the Linköping University Electronic Press and its procedures for publication and for assurance of document integrity, please refer to its www home page: <http://www.ep.liu.se/>